

USING SYNTHETIC SATELLITE IMAGES FOR AUTOMATIC MONITORING OF NWP FIELDS: OPERATIONAL APPLICATIONS

B. K. Reichert, C. Träger-Chatterjee and J. Asmus

Deutscher Wetterdienst
Kaiserleistrasse 42, 63067 Offenbach, Germany

ABSTRACT

Within the new meteorological workstation project NinJo, a comprehensive Automatic Monitoring and Alerting system (AutoMON) has been introduced at the Deutscher Wetterdienst (DWD). This system is able to permanently monitor significant weather situations in observations and model forecasts, and it automatically alerts the forecaster in case of critical (hazardous) weather events. Furthermore, it monitors the quality of Numerical Weather Prediction (NWP) fields in comparison to observations using various techniques.

Synthetic satellite images are generated from the nonhydrostatic Limited-Area Model LME of the DWD using a process-based modelling approach. The approach is based on the radiative transfer model code RTTOV-7 developed at the European Centre for Medium Range Weather Forecasts (ECMWF). Infrared (10.8 μm) and Water Vapour (6.2 μm) channels as they would be seen by the Meteosat-8 SEVIRI radiometers are used as calculated from LME using profiles of pressure, temperature, specific humidity, cloud liquid water, cloud ice, cloud cover, ozone, and some surface properties.

Within AutoMON, synthetic satellite images allow a large-scale evaluation of the quality of vertically integrated NWP model output against observations. Operational applications for the automatic and objective comparison of synthetic and observed Meteosat-8 satellite images as developed at the DWD are presented. In order to quantify deviations between synthetic and actual satellite images, statistical and image comparison techniques are used. Difference images, correlation between images, and a field of displacement vectors are calculated. The forecaster is automatically alerted in case a predefined level of disagreement between synthetic model output and the latest observed satellite image is reached. The comparison products can be displayed along with highlighted differences, correlations, and displacements. The system is demonstrated based on selected weather episodes.

Calculation of such deviations and tracking of the development of deviations with time allows an immediate assessment about which model run is closest to reality and may therefore be most reliable for the next hours considering the current observational situation. The system therefore helps the meteorologist to evaluate the quality of simulations with respect to their value for the current weather forecast. Weather situations that may develop in a way that has not been predicted by models can be recognised at an early stage.

1. INTRODUCTION

The operational numerical weather prediction system at the Deutscher Wetterdienst (DWD) currently consists of two models, the Global Model GME and the Limited-Area Model LME. The Global Model GME is an icosahedral-hexagonal grid point model with a horizontal mesh size of approximately 60 km and a vertical resolution of 31 layers. At hourly intervals, it provides boundary values for the nonhydrostatic Limited-Area Model LME with a horizontal resolution of approximately 7 km and 40 vertical layers. The LME model allows short range weather forecasting for the whole of Europe.

In cooperation with the German Space Research Centre (DLR, Institute for Physics of the Atmosphere), the Deutscher Wetterdienst (DWD) has implemented the radiative transfer model RTTOV-7 for the computation of synthetic satellite images from NWP models, currently generating images from the Model LME (Figure 1). RTTOV-7 simulates IR and WV channels of Meteosat-8 SEVIRI radiometers forced by gridpoint fields of the LME.

The effort is part of a comprehensive Automatic Monitoring and Alerting System (AutoMON) that has been developed at the DWD. This system is able to permanently monitor significant weather situations and the performance of NWP models with respect to observations. Within this context, synthetic satellite images allow vertically integrated large-scale spatial comparisons between NWP model forecasts and reality.

2. GENERATION OF SYNTHETIC SATELLITE IMAGES

Synthetic satellite images are an indicator for the vertically integrated state of the atmosphere as predicted by NWP models.

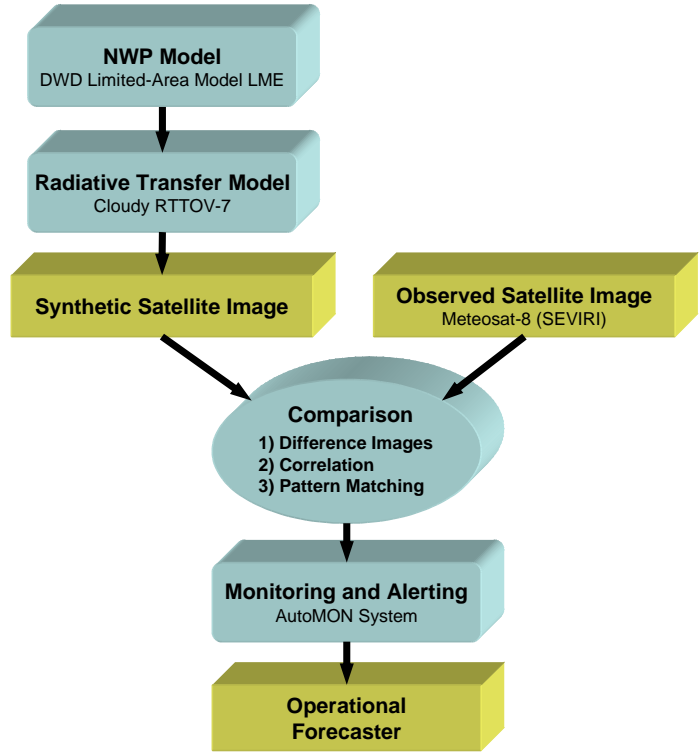


Fig. 1: General Strategy

2.1 The RTTOV-7 Model

Using the radiative transfer model RTTOV-7, microwave and infrared radiation as well as brightness temperatures can be simulated as it would be seen by the MVIRI or the SEVIRI radiometer on board of the METOSAT-7 and METEOSAT-8 satellite, respectively. As input variables, the RTTOV-7 needs the following parameters provided by LME: temperature, specific humidity, cloud liquid water, cloud ice water, cloud cover, pressure, surface pressure, skin temperature, 2-meter temperature, 2-meter specific humidity, and land-sea mask. The following approximation of the top of atmosphere upwelling radiance is used [Saunders, 2002]:

$$L(\mathbf{n}, \Theta) = (1 - N)L^{Clr}(\mathbf{n}, \Theta) + NL^{Cld}(\mathbf{n}, \Theta)$$

The radiance for clear sky conditions is simulated as:

$$L^{Clr}(\mathbf{n}, \Theta) = t_s(\mathbf{n}, \Theta) e_s(\mathbf{n}, \Theta) B(\mathbf{n}, T_s) + \int_{t_s}^1 B(\mathbf{n}; T) dt + (1 - e_s(\mathbf{n}, \Theta)) t_s^2(\mathbf{n}, \Theta) \int_{t_s}^1 \frac{B(\mathbf{n}, \Theta)}{t^2} dt$$

The radiance for cloudy sky conditions is expressed as:

$$L^{cld}(\mathbf{n}, \Theta) = t_{cld}(\mathbf{n}, \Theta) B(\mathbf{n}, T_{cld}) + \int_{t_{cld}}^1 B(\mathbf{n}, T) dt$$

with

- τ_s : surface to space transmittance
- ε_s : surface emissivity over water surfaces
- $B(\mathbf{n}, T)$: Planck function for frequency ν at temperature T
- $\tau_{cld}(\mathbf{n}, \Theta)$: cloud top to space transmittance
- T_{cld} : cloud top temperature
- \mathbf{n}, Θ : frequency \mathbf{n} , viewing angle Θ from zenith at the surface
- N : fractional cloud cover

Figure 2 shows an example for a synthetic satellite image using LME-output and the corresponding observed image.

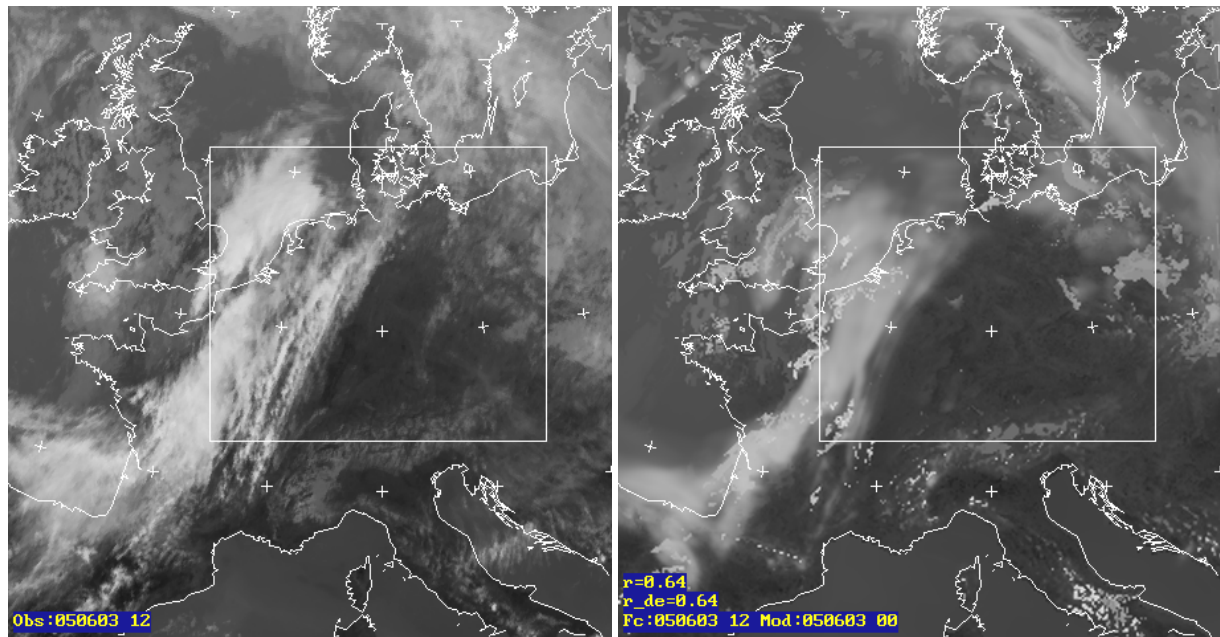


Fig. 2: Simulated satellite image over Europe for the 10.8 μm channel of Meteosat-8 using LME-output (right; 12h forecast) and the corresponding observed image (left) for June 3rd, 2005, 12.00 UTC.

2.2 Main Limitations of RTTOV-7

- RTTOV-7 only simulates top of the atmosphere radiances from a nadir or off-nadir view which intersects the Earth's surface (i.e. no limb paths)
- RTTOV-7 does not include any reflected solar component
- RTTOV-7 does not include scattering effects
- RTTOV-7 only allows for water vapour and ozone to be variable gases with all others included in the mixed gas transmittance calculation [Matricardi et al., 2001]
- The accuracy of simulations for very broad channels (e.g. SEVIRI channel 4 at 3.9 microns) is poor, significant biases (1-2K) have been noted. This is the case for all versions of RTTOV [Saunders, 2002; Keil & Tafferner, 2003]

3. EVALUATING NWP MODEL PERFORMANCE USING SYNTHETIC SATELLITE IMAGES

In order to evaluate large-scale NWP model performance, synthetic and observed satellite images are compared. An hourly (“real-time”) comparison for IR- (10.8 µm) and WV- (6.2 µm) channels for the ensemble of all LME model runs available at the observation time is performed as soon as a new observed satellite image arrives. A separate comparison for the entire LME area and a smaller section around Germany (white box in Figure 1) is calculated. The following parameters are permanently monitored by the DWD “AutoMON” system:

3.1 RMSE (Difference Images for visualisation)

The two-dimensional RMSE over the entire image is calculated and serves as a warning parameter for the AutoMON monitoring system. In addition, in order to provide a visualisation to the forecaster, differences between pixel values of the observed image and the corresponding synthetic image are calculated. The results are displayed as an overlay on top of the observed satellite image (Figure 3). Pixels of the difference image with values lying within a defined interval of allowance (in this case ± 25 K) are not coloured (i.e. no large difference between synthetic and observed image). White areas indicate that temperatures in the synthetic satellite image are too high indicating a lack of clouds in the NWP model. Black areas indicate that temperatures in the synthetic satellite image are too low indicating an excess of clouds in the NWP model.

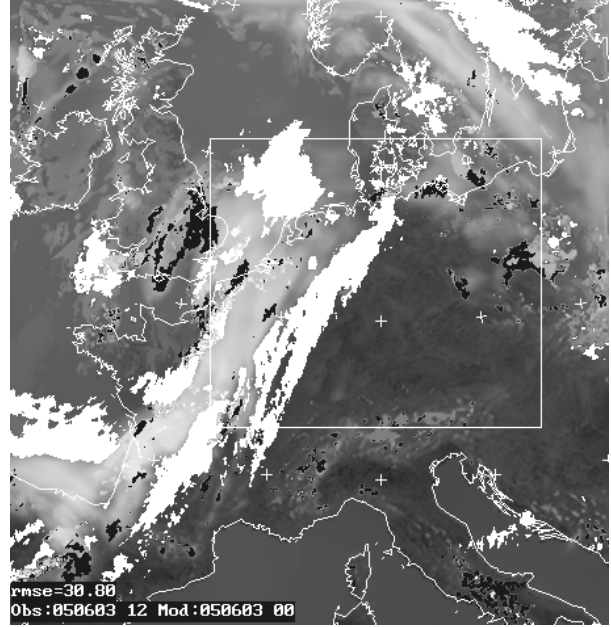


Fig. 3: Difference image showing too high (white areas) and too low (black areas) temperatures in the synthetic satellite image.

3.2 Correlation Coefficient

The correlation coefficient r for the pair of images is used as another warning parameter. It is calculated as:

$$r = \frac{\sum (x_i - \bar{x})(y_i - \bar{y})}{\sqrt{\sum_{i=1}^n (x_i - \bar{x})^2 \sum_{i=1}^n (y_i - \bar{y})^2}}$$

where

x : pixel values of the synthetic image
 y : pixel values of the observed image
 n : number of pixels in image

For each image pair one correlation coefficient is computed.

3.3 Displacement Vectors

Using a pattern-matching technique, the displacement of cloud-clusters between the synthetic and the

observed image is calculated (Figure 4). The image is divided into squares of defined size. For these squares a best match is searched in the local neighbourhood of the same position in the second image, using a pattern matching technique. The local neighbourhood is an area of defined size, configurable by the user. The size of this area also determines the maximum possible displacement vector [CineSat Software User Manual V2.6, 2001].

In order to obtain a comparison-parameter, the normalised cumulative vector-length for the entire image has been calculated. In the ideal case, i.e. the forecast exactly meets the actual state of the atmosphere, there would be no displacement between the observed and the synthetic satellite image with a parameter value of zero. However, practice has shown that this parameter is not working well in operational usage. The approach has sometimes problems to separate between features that are simply spatially shifted and features that actually don't exist in the synthetic images. The false alarm rate has been too high. Therefore, the calculated parameter is not used as a warning parameter in the automatic monitoring and alerting system. However, the displacement vectors still serve as an important visual aid for the forecaster.

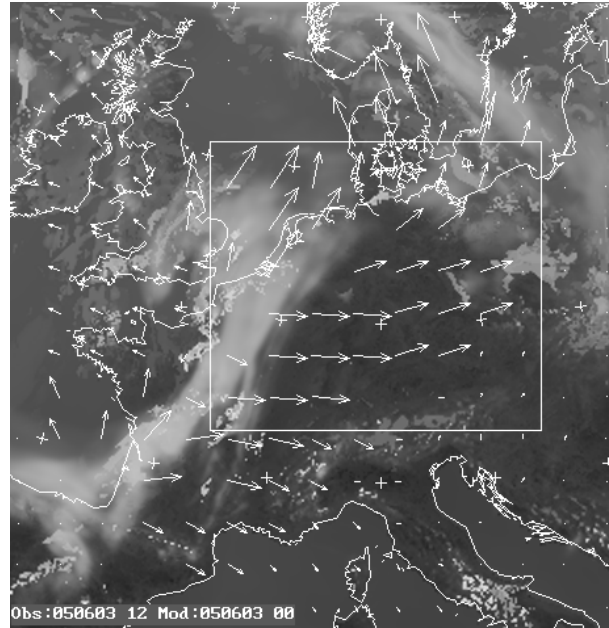


Fig. 4: Displacement from synthetic to observed satellite image.

4. OPERATIONAL USAGE: MONITORING THE QUALITY OF LME USING SYNTHETIC SATELLITE IMAGES WITHIN AUTOMON

4.1 Integration in NinJo

AutoMON is an integral part of the java-based meteorological workstation system NinJo [Koppert, 2002] that has been developed at the DWD in co-operation with its partners, the Geophysikalischer Beratungsdienst der Bundeswehr, MeteoSwiss, the Danmarks Meteorologiske Institut, and the Meteorological Service of Canada. NinJo supports the entire meteorological process and allows an integrated 2D- und 3D-visualisation of meteorological data including satellite data. It allows for an automatic monitoring and warning management using observational, nowcasting, model, and satellite data.

AutoMON automatically detects warning events and alerts the forecaster. Figure 5 gives an insight into the Graphical User Interface of AutoMON as applied to synthetic satellite images. Here, AutoMON permanently monitors the forecast model performance, in this case deviations between synthetic and observed satellite images. The meteorologist is alerted as soon as one of the parameters described above (quantifying deviations between model forecast and reality) exceeds (RMSE) or falls below (correlation) a defined threshold value. Using the Graphical User Interface, the observed deviations can be further examined. This can help to recognise weather situations that may develop in a way that has not been predicted by models at an early stage.

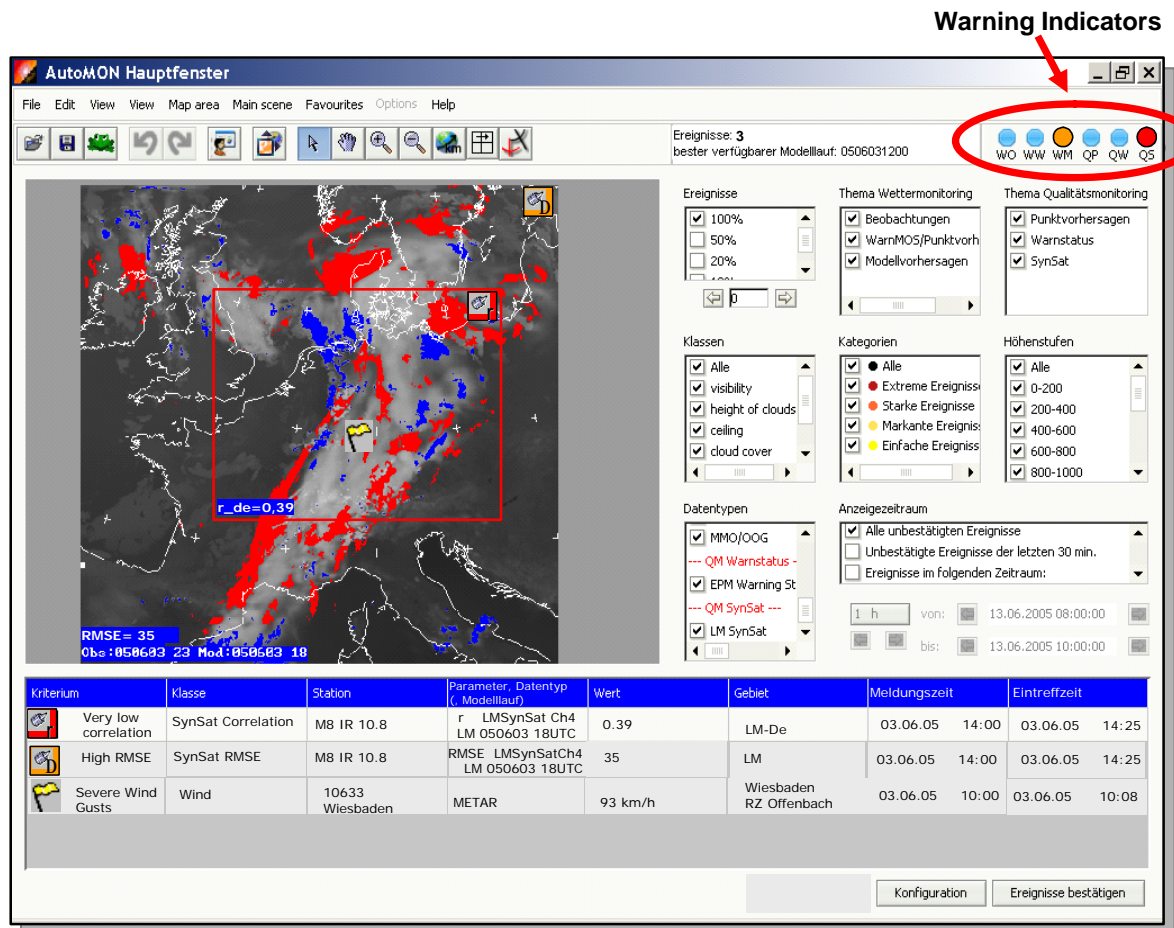


Fig. 5: NinJo - Graphical User Interface AutoMON applied to QualiSAT

4.2 Definition of Threshold Values

Comparing synthetic with observed satellite images, it is essential to define reasonable threshold values for the generation of alerting events. On one hand all major critical events should be recognised, on the other hand the false alarm rate needs to be as low as possible.

Figure 5 shows the course of correlation and RMSE between observed and simulated satellite images for the infrared (10.8 μm) channel for the time period June to September 2005. In order to find reasonable threshold values for event generation, the corresponding histograms are plotted (Figure 6). Two levels for warning events are created such that "strong events" (very low correlation / very high RMSE) occur in about 3% and "regular events" (low correlation / high RMSE) occur in about 15% of all comparisons. This means that for "strong events" ("regular events") the correlation needs to fall below 0.4 (0.5) or RMSE needs to exceed 17.5K (15K). In AutoMON it is also possible to define a combination between the two parameters for event generation.

Correlation and RMSE (Observed/Simulated) Thresholds for Alerting-Events

Correlation Events:

Low Corr: $r < 0.5$
Very low Corr: $r < 0.4$

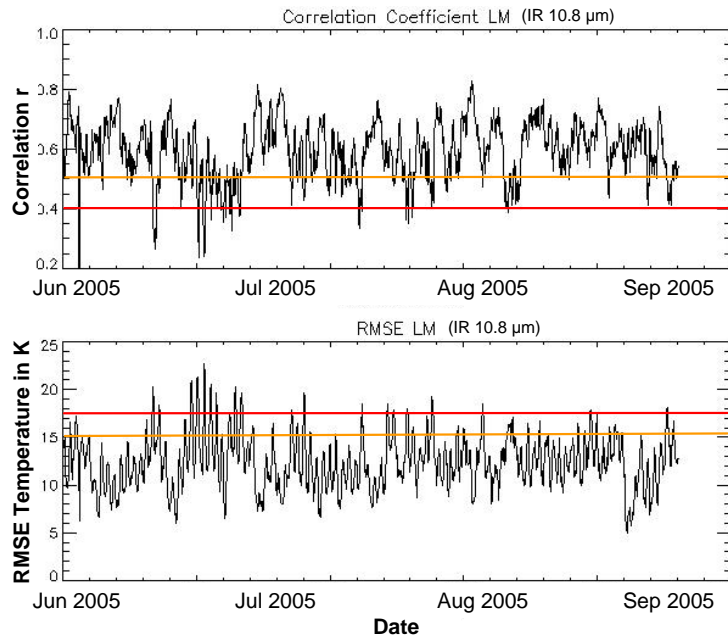
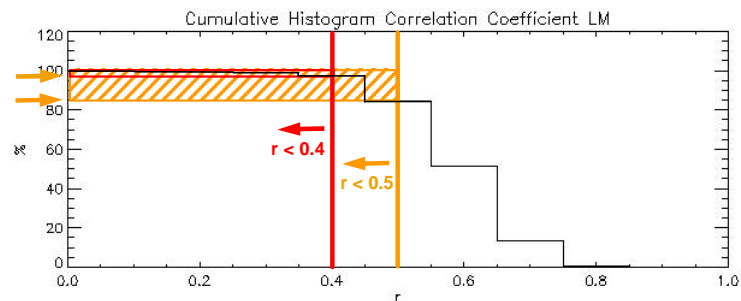


Fig. 6: Correlation (Top) and RMSE (Bottom) between observed and simulated satellite images for the infrared (10.8 μm) channel over the time period June to September 2005.

Histograms of Correlation and RMSE Thresholds for Alerting-Events

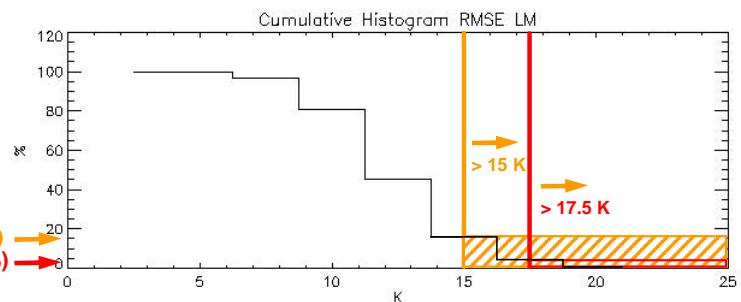
Correlation Events:

Very low Corr: $r < 0.4$ (3%)
Low Corr: $r < 0.5$ (15%)



RMSE Events:

High RMSE: $> 15 \text{ K}$ (15%)
Very High RMSE: $> 17.5 \text{ K}$ (3%)



4.3 Example: Severe Thunderstorms June 2005

Figure 8 shows the observed and simulated satellite images for a severe thunderstorm situation with hazardous rain in parts of southern Germany on 23 June 2005 (19 UTC). The synoptic situation was not sufficiently well represented by LM and weather warnings could only be issued at a very late stage using other available nowcasting information. Our approach showed strong warning indicators for a disagreement between model and observations: the correlation was as low as 0.24, RMSE was as high as 22.64 K. These values were sufficient to reach the threshold values and could have alerted the forecaster for the unpredicted weather situation some hours in advance.

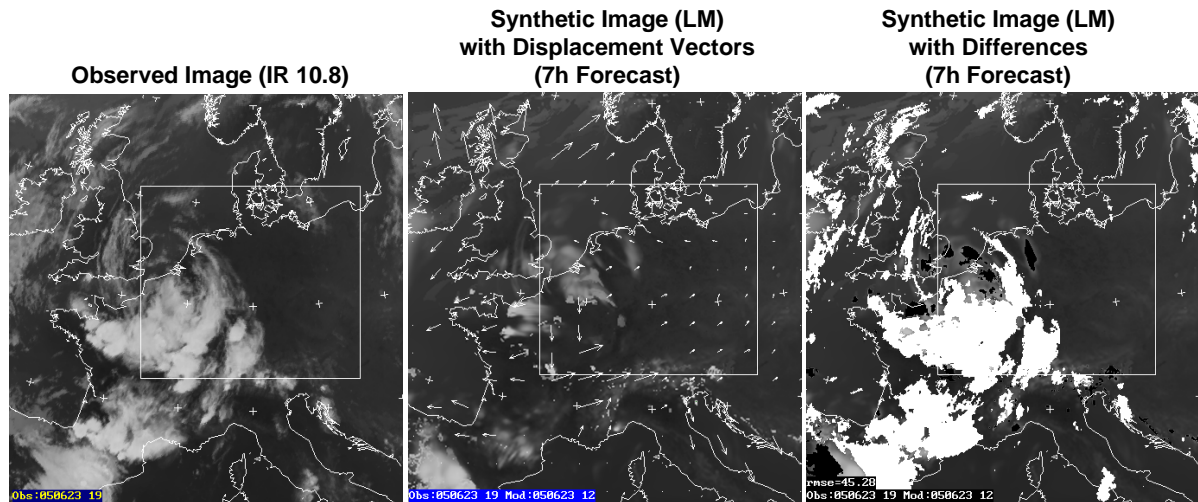


Fig. 8: Observed (left) and synthetic satellite Images for 23 June 2005 with displacement vectors (middle) and difference highlighting (right).

5. SUMMARY AND CONCLUSIONS

Synthetic satellite images are generated from the Limited Area Model LME of DWD using the radiative transfer model RTTOV-7. They are automatically compared to the latest observed satellite images in order to evaluate NWP Model performance. RMSE and correlation coefficients between the images are used to quantify deviations and they are permanently monitored for alerting events. Difference images and displacement vectors are used as visualisation aids.

The comparison of NWP-generated synthetic satellite images with observed satellite images using the described techniques allows a large-scale “real-time” evaluation of the LME model for the forecaster. Within the Framework of AutoMON as integral part of the meteorological workstation NinJo, the forecaster is immediately alerted in case of large model deviations. This can help the forecaster to evaluate the quality of simulated model fields with respect to their value for the current weather forecast. It can also help to recognize weather situations that may develop in a way unpredicted by models at an early stage.

Future work will concentrate on the investigation of the skill of the water vapour channels within our approach. It is also planned to use the method to determine the best out of the ensemble of all available model runs at a specific observation time.

6. REFERENCES

- Gepard GmbH (2001): CineSat Software User Manual Release V2.6, Vienna, Austria.
- Keil, C., and A. Tafferner (2003): LMSynSat User's Guide, unpublished.
- Koppert, H.-J. (2002): A Java-based meteorological workstation, 18th International Conference on Interactive Information and Processing Systems for Meteorology, Oceanography, and Hydrography, American Meteorological Society, p. 307-310.
- Matricardi, M., Chevallier, F., and S. Tjemkes (2001): An improved fast radiative transfer model for the assimilation of radiance observations. ECMWF Technical Memorandum 345.
- Saunders, R. (2002): RTTOV-7 User's Guide, EUMETSAT.
- Träger, C., and B. K. Reichert (2004): NinJo Functional Specification AutoMON - Automatic Monitoring and Alerting for NinJo, Part 3: Quality Monitoring Using Synthetic Satellite Images (QualiSAT), unpublished.